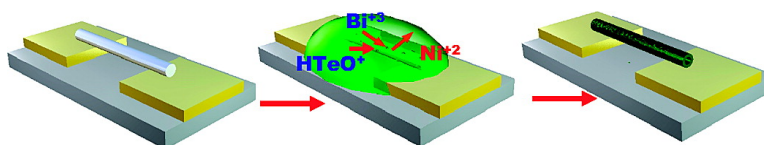


## Synthesis of BiTe Nanotubes by Galvanic Displacement

Feng Xiao, Bongyoung Yoo, Kyu Hwan Lee, and Nosang V. Myung

*J. Am. Chem. Soc.*, **2007**, 129 (33), 10068-10069 • DOI: 10.1021/ja073032w • Publication Date (Web): 27 July 2007

Downloaded from <http://pubs.acs.org> on February 15, 2009



### More About This Article

Additional resources and features associated with this article are available within the HTML version:

- Supporting Information
- Links to the 4 articles that cite this article, as of the time of this article download
- Access to high resolution figures
- Links to articles and content related to this article
- Copyright permission to reproduce figures and/or text from this article

[View the Full Text HTML](#)



## Synthesis of Bi<sub>2</sub>Te<sub>3</sub> Nanotubes by Galvanic Displacement

Feng Xiao,<sup>†</sup> Bongyoung Yoo,<sup>†</sup> Kyu Hwan Lee,<sup>‡</sup> and Nosang V. Myung<sup>\*†</sup>

Department of Chemical and Environmental Engineering, University of California-Riverside, Riverside, California 92521, and Electrochemical Processing Group, Korea Institute of Machinery and Materials, Changwon-Si, Kyungnam, 641-010, Korea

Received May 8, 2007; E-mail: myung@enr.ucr.edu

Thermoelectric (TE) energy converters are solid-state devices that can generate electricity by harvesting waste thermal energy, thereby improving the efficiency of a system. The many advantages of TE devices include solid-state operation, zero-emissions, vast scalability, no maintenance, and a long operating lifetime. Nonetheless, because of their limited energy conversion efficiencies, thermoelectric devices currently have a rather limited set of applications. However, there is a reinvigorated interest in the field of thermoelectrics by identifying classical and quantum mechanical size effects, which provide additional ways to enhance energy conversion efficiencies in nanostructured materials<sup>1,2</sup> including superlattice thin films<sup>3</sup> and quantum dots.<sup>4</sup> For example, thermoelectric figure of the merit (ZT) up to 2.5 was achieved by synthesizing two-dimensional Sb<sub>2</sub>Te<sub>3</sub>/Bi<sub>2</sub>Te<sub>3</sub> superlattice thin films, exceeding previous limits of ~1 from bulk counterpart.<sup>5</sup> Even more exciting are the theoretical predictions for one-dimensional nanostructures including nanowires and nanotubes, which are thought to have ZT exceeding 5.<sup>1,6</sup> In the case of nanotubes, theoretical calculation predicts a further reduction in the thermal conductivity, because of a stronger phonon-surface scattering, compared to solid nanowire.<sup>7</sup>

Limited works have been reported on the synthesis of thermoelectric nanotubes including hydrothermally grown Bi, Bi<sub>2</sub>Se<sub>3</sub>, and Bi<sub>2</sub>Te<sub>3</sub> nanotubes<sup>8</sup> and electrodeposited Bi nanotubes.<sup>9</sup> However, these processes have some limitations. For example, the nanotube production yield is very low (<30%).<sup>8</sup> In the template-directed method it is difficult to restrict the proceeding electrodeposition along the walls without filling up the whole pores.<sup>9</sup>

The galvanic displacement reaction is an electrochemical process, which is induced by the difference in redox potentials between materials. Various metallic nanotubes have been synthesized via this reaction (e.g., gold nanotubes from silver nanowires);<sup>10</sup> however, no one to-date has demonstrated the synthesis of semiconducting thermoelectric nanotubes. In this paper, we demonstrate the synthesis of high-aspect ratio Bi<sub>2</sub>Te<sub>3</sub> nanotubes with controlled composition by galvanic displacement of nickel nanowires in acidic nitric electrolyte containing Bi<sup>3+</sup> and HTeO<sub>2</sub><sup>+</sup> ions. Bi<sub>2</sub>Te<sub>3</sub> nanotubes were synthesized because Bi<sub>2</sub>Te<sub>3</sub> and its derivative compounds are considered to be the best materials used in thermoelectric refrigeration at room temperature. In addition to synthesis, we also demonstrate the fabrication method to create individual Bi<sub>2</sub>Te<sub>3</sub> nanotube-based devices by combining the magnetic assembly of single nickel nanowire across microfabricated electrodes, followed by a galvanic displacement reaction.

Figure 1A shows the schematic illustration of the galvanic displacement reaction of Ni nanowires to Bi<sub>2</sub>Te<sub>3</sub> nanotubes. The detailed experimental conditions are provided in the Supporting Information. When Ni nanowires are immersed into an acidic nitric solution containing Bi<sup>3+</sup> and HTeO<sub>2</sub><sup>+</sup> ions, Ni nanowires are

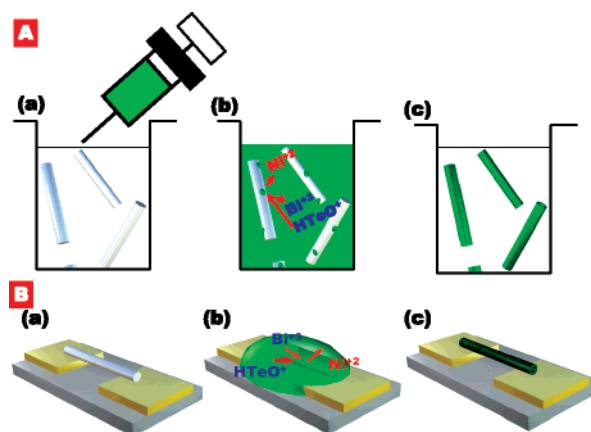


Figure 1. Schematic illustrations of Bi<sub>2</sub>Te<sub>3</sub> nanotube synthesis (A) and individual Bi<sub>2</sub>Te<sub>3</sub> nanotube laid across electrodes (B).

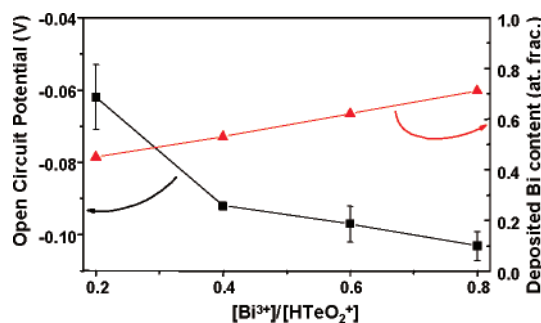


Figure 2. Dependence of the steady-state OCP and the deposited Bi content in nanotubes on the ratio of [Bi<sup>3+</sup>]/[HTeO<sub>2</sub><sup>+</sup>].

galvanically displaced to form Bi<sub>2</sub>Te<sub>3</sub>, because of the difference in the reduction potentials (i.e., Ni<sup>2+</sup>/Ni<sup>0</sup> ( $E^{\circ} = -0.257$  V vs SHE) and Bi<sup>3+</sup>, HTeO<sub>2</sub><sup>+</sup>/Bi<sub>2</sub>Te<sub>3</sub> ( $E^{\circ} = -0.62$  V - 0.01475 log[HTeO<sub>2</sub><sup>+</sup>] = 0.0443 [pH] vs NHE)).<sup>11,12</sup>

To monitor the reaction, the open-circuit potential (OCP) of nickel thin films deposited on platinum was first measured continuously, while immersed in an acidic nitric solution (1 M HNO<sub>3</sub>) containing 0.002–0.008 M Bi<sup>3+</sup> and 0.01 M HTeO<sub>2</sub><sup>+</sup> (Figure S.1 in Supporting Information). In general, the OCP sharply decreased to a steady-state value. When nickel thin films were completely displaced by Bi<sub>2</sub>Te<sub>3</sub> films, the OCP was increased to >0 V versus SCE. The deposition time was ~60 min at [Bi<sup>3+</sup>] = 0.002 M and reduced to ~30 min when [Bi<sup>3+</sup>] = 0.008 M. Figure 2 shows the dependence of steady-state OCP and the deposited Bi content in nanotubes on the [Bi<sup>3+</sup>]/[HTeO<sub>2</sub><sup>+</sup>] ratio. As expected, the OCP of nickel films decreased with an increase in the ratio of [Bi<sup>3+</sup>]/[HTeO<sub>2</sub><sup>+</sup>].

<sup>†</sup> University of California-Riverside.

<sup>‡</sup> Korea Institute of Machinery and Materials.

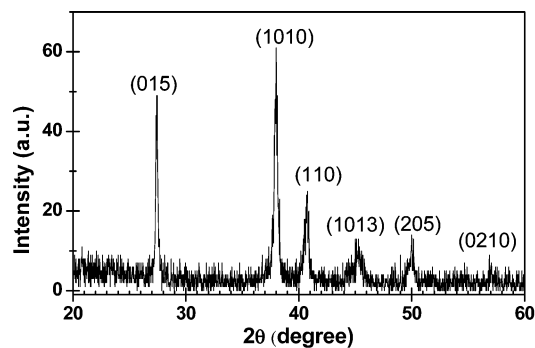


**Figure 3.** XRD pattern of galvanically displaced  $\text{Bi}_2\text{Te}_3$  from Ni ( $3\ \mu\text{m}$ )/Si in the solution of  $0.01\ \text{M}\ \text{HTeO}_2^+$ ,  $0.006\ \text{M}\ \text{Bi}^{3+}$ , and  $1\ \text{M}\ \text{HNO}_3$ .

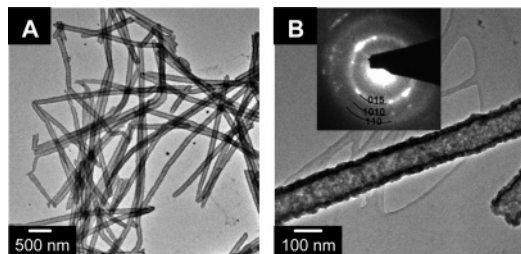
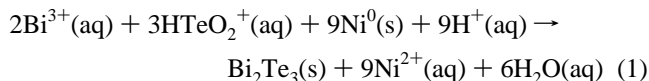


**Figure 4.** TEM images and SAED pattern of high aspect ratio  $\text{Bi}_2\text{Te}_3$  nanotubes (A) synthesized from nickel nanowire ( $\sim 100\ \text{nm}$  in diameter). Tube thickness was approximately  $20\ \text{nm}$  (B).

The X-ray diffraction pattern of the deposited film confirmed the formation of highly crystalline rhombohedral  $\text{Bi}_2\text{Te}_3$  crystals without obvious preferential orientation (Figure 3).

On the basis of the thin film results, continuous  $\text{Bi}_2\text{Te}_3$  nanotubes were synthesized by displacing electrodeposited nickel nanowires ( $100\ \text{nm}$  in diameter) in solution containing  $0.002\text{--}0.008\ \text{M}\ \text{Bi}^{3+}$  and  $0.01\ \text{M}\ \text{HTeO}_2^+$ . The deposited Bi content in the nanotubes varied linearly with the ratio (Figure 2), which are in good agreement with those observed by Stacy et al.<sup>12</sup> They observed that nearly stoichiometric  $\text{Bi}_2\text{Te}_3$  thin films were electrodeposited when the applied potentials were more negative than ca.  $-0.08\ \text{V}$  versus SCE. They concluded that the direct deposition of  $\text{Bi}_2\text{Te}_3$  is thermodynamically favorable over co-deposition of elemental  $\text{Bi}^0$  and  $\text{Te}^0$  metals because of negative Gibbs free energy of  $\text{Bi}_2\text{Te}_3$  formation ( $\Delta G_f^0 = -899.088\ \text{kJ/mol}$ ).<sup>12</sup> Thus, the galvanic displacement reaction of nickel nanowires to  $\text{Bi}_2\text{Te}_3$  nanotubes can be represented as follows:



Figures S.2 and 4 show the SEM and TEM images of synthesized  $\text{Bi}_2\text{Te}_3$  nanotubes from a solution containing  $0.006\ \text{M}\ \text{Bi}^{3+}$ . Evidence for  $\text{Bi}_2\text{Te}_3$  nanotube formation is also confirmed with the selected-area electron diffraction (SAED) pattern (inset image of Figure 4B). Ni trace was not observed by both EDAX (Figure S.3) and atomic absorption spectroscopy (AAS) analysis. The surface of nanotubes was rough which might be caused by rough Ni nanowires. Homogeneous  $\text{Bi}_2\text{Te}_3$  nanotubes with well-defined void spaces were formed, probably because the displacement reaction occurred initially at the spots with highest surface energy and then proceed to those with lower energies. As a result, an incomplete

thin sheath formed at the early stage allowing both reactants and products to diffuse across the sheath until a homogeneous  $\text{Bi}_2\text{Te}_3$  nanotube is formed.

To fabricate nanodevices, nanotubes must be integrated with micro- or macroelectrodes. We achieved this goal by first magnetically assembling an individual nickel nanowire on gold electrodes (Figure 1Ba), followed by postannealing in a reducing environment ( $5\% \text{H}_2 + 95\% \text{N}_2$ ) at  $500\ ^\circ\text{C}$  for 2 h to create interconnect with minimum contact resistance.<sup>13</sup> Once a good electrical contact was made between nanowire and electrodes, the nickel nanowire was displaced to form  $\text{Bi}_2\text{Te}_3$  nanotubes (Figure 1Bb,c). Finally, the electrodes and nanotubes were rinsed thoroughly with DI water. Using this device, temperature-dependent electrical properties of  $\text{Bi}_2\text{Te}_3$  nanotubes were measured. Figure S.4, parts a and b show the temperature-dependent current–voltage ( $I$ – $V$ ) curves and resistances. Ohmic contacts were formed between the nanotube and electrodes as indicated by the linear characteristic of the  $I$ – $V$  curves. Figure S.4b shows that the nanotube was a semiconductor.

In summary, we synthesized stoichiometric  $\text{Bi}_2\text{Te}_3$  nanotubes by a galvanic displacement reaction of Ni nanowires. The composition of  $\text{Bi}_2\text{Te}_3$  nanotubes was precisely tuned by adjusting the  $[\text{Bi}^{3+}]/[\text{HTeO}_2^+]$  ratio. The ability to adjust the composition is critical since optimum n-type (Bi-doped  $\text{Bi}_2\text{Te}_3$ ) and p-type (Te-doped  $\text{Bi}_2\text{Te}_3$ ) nanotube can be synthesized by altering the ratio. By combining the premagnetically assembled nickel nanowire and galvanic displacement reaction, individual  $\text{Bi}_2\text{Te}_3$  nanotube-based devices were fabricated and their temperature-dependent electrical properties were measured.

**Acknowledgment.** We greatly acknowledge the support of this work by funding from KIMM.

**Supporting Information Available:** Experimental details, SEM, EDS, and temperature-dependent  $I$ – $V$  characteristics of nanotubes are available. This material is available free of charge via the Internet at <http://pubs.acs.org>.

## References

- Hicks, L. D.; Dresselhaus, M. S. *Phys. Rev. B* **1993**, *47*, 12727.
- Mahan, G. D.; Lyon, H. B. *J. Appl. Phys.* **1994**, *76*, 1899.
- Koga, T.; Sun, X.; Cronin, S. B.; Dresselhaus, M. S. *Appl. Phys. Lett.* **1999**, *75*, 2438.
- Harman, T. C.; Taylor, P. J.; Walsh, M. P.; LaForge, B. E. *Science* **2002**, *297*, 2229.
- Venkatasubramanian, R.; Siivola, E.; Colpitts, T.; O'Quinn, B. *Nature* **2001**, *413*, 597.
- Lin, Y. M.; Sun, X. Z.; Dresselhaus, M. S. *Phys. Rev. B* **2000**, *62*, 4610.
- Yang, R.; Chen, G.; Dresselhaus, M. S. *Nano Lett.* **2005**, *5*, 1111.
- (a) Li, Y. D.; Wang, J. W.; Deng, Z. X.; Wu, Y. Y.; Sun, X. M.; Yu, D. P.; Yang, P. D. *J. Am. Chem. Soc.* **2001**, *123*, 9904. (b) Cui, H. M.; Liu, H.; Li, X.; Wang, J. Y.; Han, F.; Zhang, X. D.; Boughton, R. I. *J. Solid State Chem.* **2004**, *177*, 4001. (c) Zhao, X. B.; Ji, X. H.; Zhang, Y. H.; Zhu, T. J.; Tu, J. P.; Zhang, X. B. *Appl. Phys. Lett.* **2005**, *86*, 062111.
- Li, L.; Yang, Y. W.; Huang, X. H.; Li, G. H.; Ang, R.; Zhang, L. D. *Appl. Phys. Lett.* **2006**, *88*, Art. No. 103119.
- (a) Sun, Y. G.; Mayers, B. T.; Xia, Y. N. *Nano Lett.* **2002**, *2*, 481. (b) Mayers, B. T.; Xia, Y. N. *Adv. Mater.* **2002**, *14*, 279. (c) Sun, Y. G.; Mayers, B. T.; Xia, Y. N. *Adv. Mater.* **2003**, *15*, 641. (d) Wen, X. G.; Yang, S. H. *Nano Lett.* **2002**, *2*, 451.
- (a) *CRC Handbook of Chemistry & Physics*; CRC Press: Cleveland, OH, 2006. (b) Xiao, F.; Yoo, B.; Ryan, M. A.; Lee, K. H.; Myung, N. V. *Electrochim. Acta* **2006**, *52*, 1101.
- Martin-Gonzalez, M.; Prieto, A. L.; Gronsky, R.; Sands, T.; Stacy, A. M. *J. Electrochem. Soc.* **2002**, *149*, C546.
- (a) Hangarter, C. M.; Myung, N. V. *Chem. Mater.* **2005**, *17*, 1320. (b) Yoo, B. Y.; Rheem, Y.; Beyermann, W. P.; Myung, N. V. *Nanotechnology* **2006**, *18*, 2512. (c) Rheem, Y.; Yoo, B. Y.; Beyermann, W. P.; Myung, N. V. *Nanotechnology* **2006**, *18*, 015202. (d) Hangarter, C. M.; Rheem, Y.; Yoo, B. Y.; Yang, E.-H.; Myung, N. V. *Nanotechnology*, **2007**, *18*, 205305.

JA073032W